

GOMOS CALIBRATION ON ENVISAT – STATUS ON DECEMBER 2002

**Gilbert Barrot⁽¹⁾, Jean-Loup Bertaux⁽²⁾, Renaud Fraisse⁽³⁾, Antoine Mangin⁽¹⁾, Alain Hauchecorne⁽²⁾,
Odile Fanton d'Andon⁽¹⁾, Francis Dalaudier⁽²⁾, Charles Cot⁽²⁾, Erkki Kyrölä⁽⁴⁾, Johanna Tamminen⁽⁴⁾,
Bertrand Théodore⁽¹⁾, Didier Fussen⁽⁵⁾, Rob Koopman⁽⁶⁾, Lidia Saavedra⁽⁶⁾, Paul Snoeij⁽⁶⁾**

⁽¹⁾ ACRI-ST,260, route du Pin Montard, Sophia-Antipolis Cedex BP 234 F-06904 FRANCE, gomval@acri.fr

⁽²⁾ Service d'Aéronomie du CNRS BP3 - 91371 - Verrières le Buisson Cedex F- FRANCE, bertaux@aerov.jussieu.fr

⁽³⁾ Astrium SAS, 31402 TOULOUSE cedex FRANCE, renaud.fraisse@astrium-space.com

⁽⁴⁾ FMI, P.O.BOX 503, FIN-00101 Helsinki FINLAND, Erkki.Kyrola@fmi.fi

⁽⁵⁾ IASB, Avenue Circulaire 3 B-1180 Brussels Belgium, Didier.Fussen@bira-iasb.oma.be

⁽⁶⁾ ESA ESTEC and ESRIN centres

ABSTRACT/RESUME

This paper summarises the status of the GOMOS calibration assessed by the GOMOS CAL/VAL team after nine months of the instrument in-flight life. The first GOMOS occultation was successfully measured on March 22, 2002, starting the calibration and verification activity phase. Since this date, more than 50000 occultations have been performed until end of 2002. The GOMOS CAL team was in charge of i) the full in-flight calibration and re-characterisation of GOMOS, ii) all the activities required to achieve the complete verification of the level 1b processing models, including: algorithms, auxiliary products, instrument performance, measurements geolocation and validation of the atmosphere related parameters. Lastly, the GOMOS CAL team provided the relevant inputs to the GOMOS mission planning monitoring, and to the future routine calibration operations and validation activities. The GOMOS instrument in-flight performances are globally very good, in line with expected budget, except for CCD behaviour (hot pixels, RTS). All measured performances are described hereafter, together with assessment methodology and recommendations.

1 GOMOS INSTRUMENT PERFORMANCE

1.1 Brief reminder of the GOMOS instrument measurement concept

The GOMOS operating principle relies on the stellar occultation method, which consists to observe a star outside the atmosphere (thus providing a reference stellar spectrum) and track it as it sets through the atmosphere (thus providing spectra with absorption features). When these occulted spectra are divided by the reference spectrum, nearly calibration-free horizontal transmission spectra are obtained, assuming the instrument response function does not change during one occultation; lasting typically 30 to 40 seconds. These transmissions provide the basis for retrieval of atmospheric constituents density profiles, which benefits from the fact that observing the star light confines the measurement to a "thin" well-defined volume.

1.2 Method

The verification of the instrument health and performance activities have started on March 22, 2002, just after the SODAP phase which had validated the correct behaviour of the Service Module, Payload Equipment Bay and Payload instruments, checked the GOMOS level 0 products format, and roughly verified that the instrument can be commanded as expected.

Due to launch and in-orbit environments, several instrument characteristics may have been modified like the instrument response function, thermal distortion and settling of the optical bench, ... and this calls for calibration and monitoring of GOMOS parameters behaviour and performance: electronic gain chain, read-out noise and offset, non linearity, dark charge, pixel response non-uniformity, radiometric sensitivity, spectral line spread function, wavelength assignment, vignetting, and straylight.

All measured performances are described hereafter. The method and tools used during the Calibration phase are briefly described. Then, the measurement results are analysed and compared to the expectations and the specifications. Finally, for each calibration parameter, recommendations are given for the routine mission.

1.3 Acquisition, detection and pointing performance

The objective is to verify if the GOMOS instrument is able to acquire and track stars outside and through the atmosphere. This task will allow to assess tracking limits (altitude range versus star magnitude) and to verify the dynamic component of the pointing errors that contribute to the dynamic spatial and spectral Line Spread Functions.

The detection and acquisition performance have been analysed:

- during SODAP, for the acquisition and tracking ranges
- by analysing the successful acquisition of faint stars

The mispointing observed during SODAP is linked with the acquisition cone. It has been analysed using the Most Illuminated Pixel position in detection given in the auxiliary data.

Tracking capability has been analysed using the SATU noise monitoring (auxiliary data) and looking at the altitude corresponding to the tracking loss.

The tools used for these analyses are mainly the Calibration software CALEX and the GOMOS processing prototype GOPR.

The acquisition range and tracking Field Of View are consistent with the delivery status. Margins have been taken in order to be sure not to hit the limits.

Table 1: Ranges and duration performance

Acquisition	expected	measured	spec
SFM range	-11 - 91° 61.7 - 69°	> -10.8 - 90.8° > 62 - 68.8°	-10 - 90° 62 - 68°
Tracking FOV	7.4°; 6.5°	> 7.1°; 5.3°	7°; 5°
Rallying speed	> 2°/s	> 2°/s	2°/s
Centring duration	8.1 s	< 7 s	10 s

The duration of rallying and centring phases are also confirmed.

For the performance in detection, a limited number of stars have been tested and the detection threshold has been kept to a safe value. Indeed, a too small value can lead to a class C anomaly which put instrument in Refuse mode. Even if there is no danger for the instrument, we decided not to test the limits of detection. Indeed, the actual number of tested stars is already much larger than the scientific need (and than the specification).

Table 2: Detection probability results

Detection capability	expected	measured	spec
Hot star dark limb	4.6	> 3.7	2.4
Cold star dark limb	6.8	> 4.5	4
Hot star bright limb	2.2	> 3.2	1.6
Cold star bright limb	4.4	> 4	3.2

Acquisition mispointing performance is the difference between expected and observed position of the star in the SATU FOV after rallying. The expected value is less than 0.16°. The observed value during SODAP is 0.3° in elevation (El) and 0.1° in azimuth (Az).

The analysis of the unexpected mispointing in Elevation has shown:

- a contribution due to a forgetting of GOMOS optical frame / GOMOS reference cube alignment in the configuration matrix (0.1° in elevation and 0.06° in azimuth).
- a possible impact of the gravity compensation of the mechanism. A shift of a few tens of microns could easily induce a bias of 0.1° in elevation.
- a possible contribution due to the calibration curves of SFA angles.

This difference has been corrected and the stars are now detected at the centre of the SATU. No trend has been observed since then (Fig. 1).

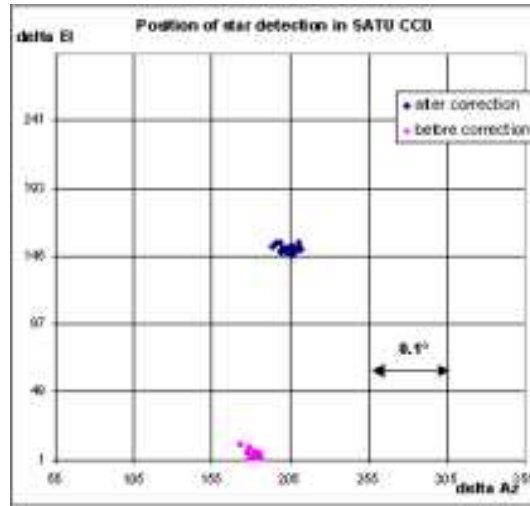


Fig. 1: Position of the detection of stars in SATU before and after the correction.

Tracking noise and robustness: the expected value of the SATU noise equivalent angle in dark limb (at 100 Hz) is 13 μrad (3 σ) for a specification of 18 μrad . The measured value is better than 3 μrad in dark limb (DL) and 10 μrad in bright limb (BL) (35 km altitude). Noise is less than 1 μrad (3 σ) for Sirius.

Fig. 2 presents the mispointing error reported by the SATU data. Movement in elevation around 100 km is due to the presence of the O₂ emission layer. The refraction effect can be seen in elevation below 40 km.

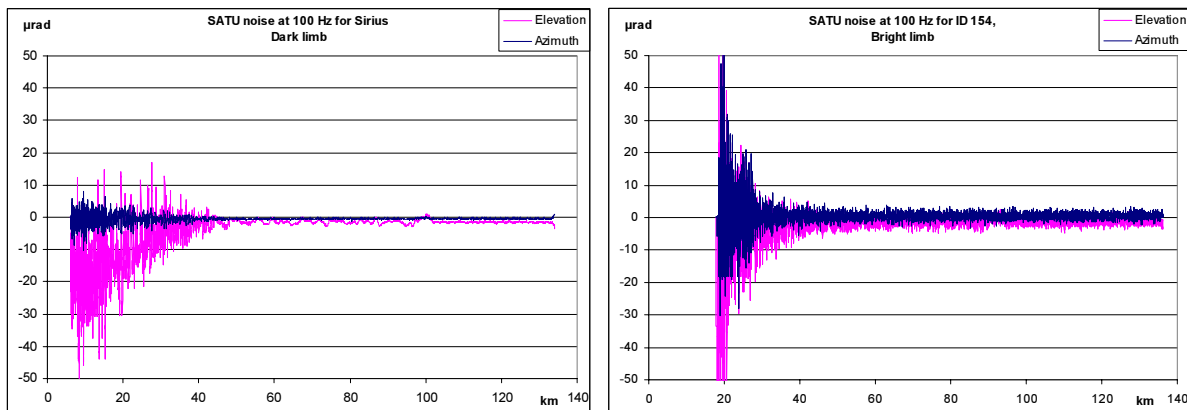


Fig. 2: SATU noise equivalent angle for two different stars in dark and bright limb

The altitude range has been analysed for many of the stars already acquired.

The average minimum altitude is 15 km in dark limb and 22 km in bright limb, better than expected. It is nearly not dependent on magnitude since the tracking loss is mainly due to the refraction and the scintillation that depend on the atmosphere conditions.

The minimum altitude reached in tracking is below 5 km for the brightest stars.

The refraction induces a displacement on the SATU up to 20 μrad at 10 km.

The effect on the spectrum (bending in UV) appears when flux is already nearly completely absorbed by atmosphere.

The values of the ranges (in acquisition/tracking) and the durations (in rallying/ centring) that have been confirmed have been implemented in the RGT Operational Parameter file. Margins have been taken with respect to the GOMOS expected capability but should be kept for the lifetime since it is already larger than the scientific need. These performances are not expected to change during the life. Only an analysis of the possible anomalies is required.

For detection, the number of stars which can be acquired is larger than 500 (already enough for the mission). The detection threshold (15 LSB) should be kept like this and should anyway not be decreased below 5 LSB since there could be a risk of a class C anomaly.

1.4 Optomechanical and thermal performance

The tool used for these analyses is mainly the CALEX calibration software.

Different instrument modes are used for these parameters:

- Analysis through spatial spread monitoring mode for the spatial displacement. The barycentre computation leads to potential adjustment of integration area size and position (band setting task). Spatial extension of the star is an indication for monitoring the defocus.
- Analysis through occultation mode for the spectral displacement (wavelength assignment). The wavelength assignment variation is computed by correlation of spectra.
- Analysis through occultation mode for the SATU/Slit displacement. We measure the comparison of total flux on each CCD when the star is artificially moved on the SATU.

The optomechanical displacements due to the launch are less than 0.3 pixels for all CCD.

The thermal influence on each of these performances has been measured during different cooling phases (from +10°C down to around -4°C). At +10°C, the thermal behaviour of GOMOS is as expected, close to the "Beginning Of Life hot" thermal case. No anomaly or curious behaviour has been observed. The variations along orbit are very consistent with the model.

Fig. 3 presents the variation of the temperature for several GOMOS elements after the last cooling phase. The variation for DMSA and DMSB (where the CCDs are) is close to 0.35°. Knowing the thermal sensitivity of the spectrometer pixels, this variation leads to an inaccuracy of 5 to 6 % on the dark charge level. As the accuracy of the thermistor measurements (coding accuracy) is also 0.40°C, the final inaccuracy may be of the order of 10 %.

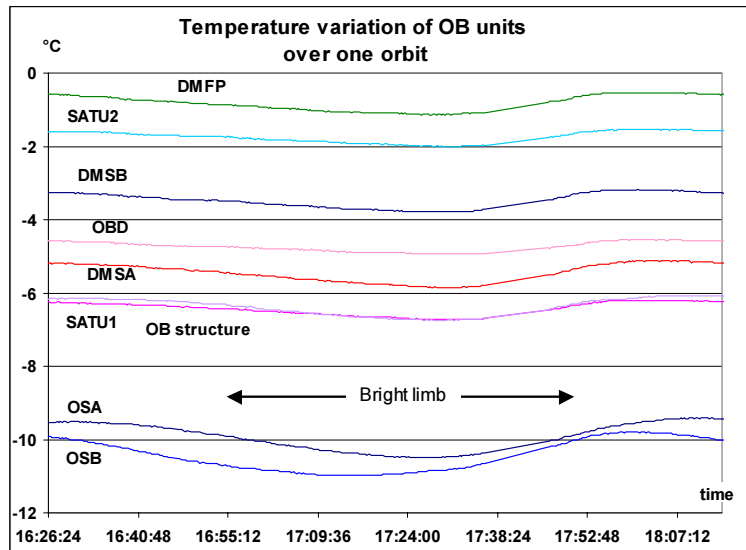


Fig. 3: Temperature variation of OB units over one orbit

The displacements with temperature variation are inside the expected budget (0.5 pixel/10°C for DMSA and 0.1 pixel for DMSB). The variation during one orbit is lower than 0.03 pixel. The spectral stability is better than expected.

The optical performance are as expected. The size of the star is included in 4 lines (at 95%).

Fig. 4 shows the size of the star spectrum image in the spatial direction. X-axis is the star flux in electrons, Y-axis is the CCD line index.

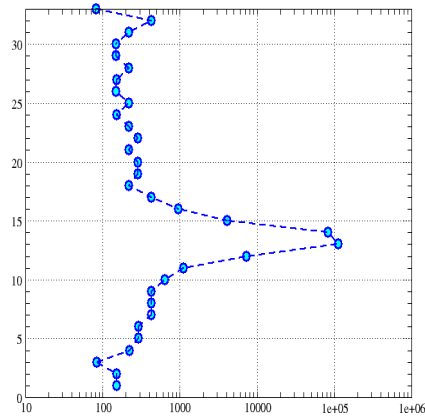


Fig. 4: Star spectrum on spectrometers CCD

The temperature and thermal stability shall be monitored every month to analyse the seasonal influence. For the band setting (spatial displacement), no trend is expected. We recommend re-characterising it every 3 months. Since there is a very low accuracy of the measurement of the defocus and that no trend is expected, we do not propose any further monitoring. For the SATU/Slit alignment, no trend is expected. We recommend re-characterising it every 6 months.

1.5 Radiometric performance

1.5.1 Non-linearity

The electronic chain linearity has been verified with measurements from GOMOS set in Monitoring Linearity Mode. Same stars have been observed with different integration times, from 0.25 s up to 10.0 s.

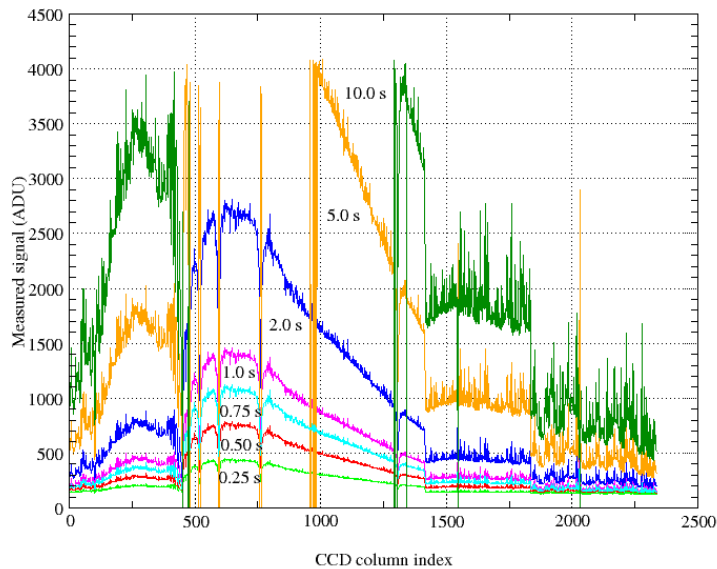


Fig. 5. : Star spectrum on spectrometers CCD

The non-linearity specification was 1% per decade. The in-flight calibration has shown an average non-linearity better than 0.4% on full dynamic range.

The electronic chain offset is also calibrated using the same measurements. The stability of the offset computed from calibrations performed at several times is better than 0.1 ADU.

1.5.2 Non-uniformity of pixel response

The pixel response non-uniformity has been measured at pixel and at band level using the Uniformity monitoring mode and the occultation fictive star mode of the GOMOS instrument. The measurements have been made in bright limb conditions.

The tools used for these analyses are mainly the calibration software CALEX.

The radiometric uniformity performance is consistent with expected. There is no degradation of the pixel response even for the pixels showing a degraded dark current.

One bad pixel in DMSA2 (-26%) already seen on ground has not moved nor degraded.

The interferences on IR spectrometers present the same shape and amplitude as on ground. Fig. 6 presents the PRNU observed on DMSB2 (IR2).

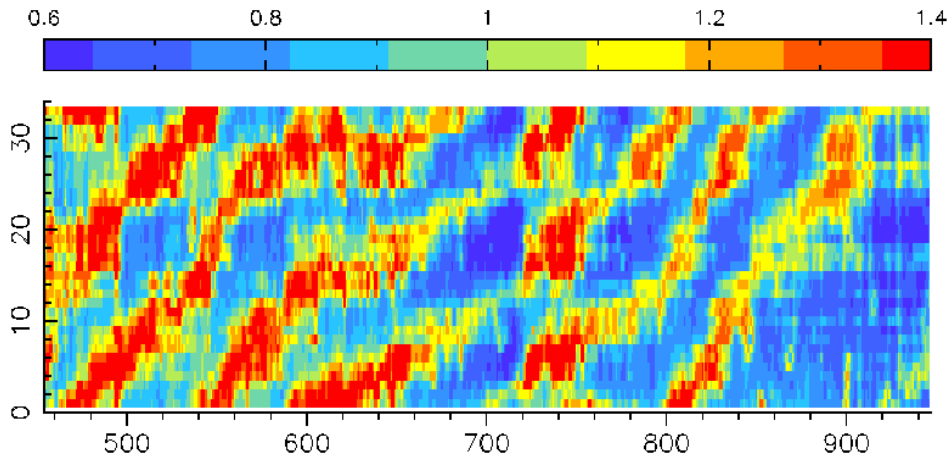


Fig. 6: Interference pattern observed on IR2 spectrometer

The slit profile measurement is consistent with ground.

Table 3: Non-uniformity results

Radiometric Uniformity	UV	VIS	IR1	IR2
mean ground	1.7%	1.7%	1.9%	12%
flight	1.4%	1.6%	2.4%	12%
max ground	3%	3.6%	6.8%	42%
flight	< 4%	4.3%	6.6%	40%

No trend has been measured yet for this parameter.

The response non-uniformity shall be monitored every month, especially in IR, where interferences position is influenced by temperature. No variation is expected if temperature is stable.

1.5.3 Radiometric calibration and stability

The radiometric calibration is performed by comparing the stellar spectra with external reference sources. Good consistency between measurements and on-ground characterisation is observed.

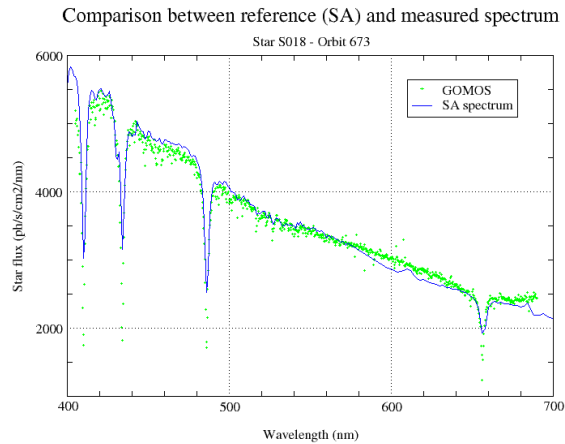


Fig. 7: Radiometric calibration

Variation level between orbits is compatible with the theoretical noise.

Very stable radiometry in all the spectral coverage of GOMOS: as a consequence, the complete spectral range of GOMOS is now considered as valid and used in the ground processing. No trend observed yet.

It should be noted that the absolute radiometric calibration has no significant impact on the level 2 products (species density profiles).

1.6 Wavelength assignment

The spectral calibration is performed by comparing the spectral assignment of several columns with external well-known reference sources (see Fig. 8). It should be noted that a vacuum wavelength scale is adopted for GOMOS. While one column per CCD becomes the *reference column*, the other calibrated columns are used to update the spectral dispersion law of the spectrometer. Lastly, the spectral assignment of any CCD column is done by using the reference column and the spectral dispersion law.

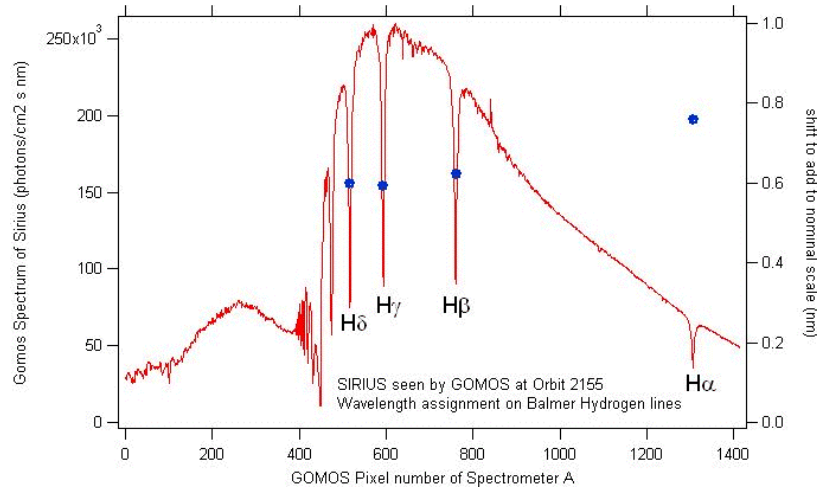


Fig. 8: Wavelength calibration

The wavelength assignment found by this method is consistent with the spectral assignment of the cross-sections used in the level 2 processing (see Fig. 9: comparison of the measured and modelled transmission at 26.6 km in SPA1 spectral range). The accuracy of the wavelength calibration is of the order of 1/30 pixel.

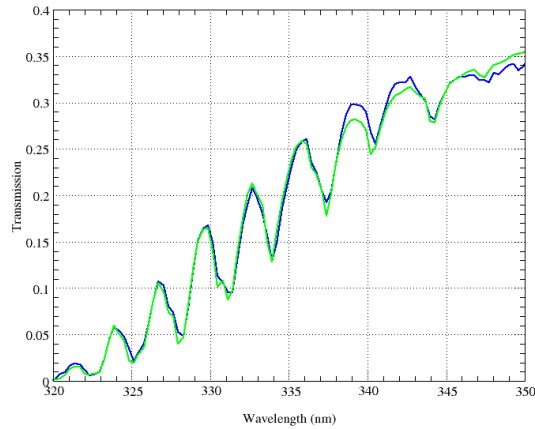


Fig. 9. : Transmission model (green) versus measured transmission (blue)

No trend has been observed during several weeks. However, due to the high sensitivity of the retrieval performance to the correctness of the wavelength assignment, this calibration shall be carefully and regularly monitored on a monthly basis.

1.7 CCD dark charge level, hot pixels, RTS

Three operations are performed for the analysis of the GOMOS CCD performance:

- Confrontation of what was expected and calibrated on-ground and what is measured in flight.
- Survey of the temporal evolution of dark charge (DC) value at pixel level and at global level using dark sky observations
- Spectral analysis (Fourier transform) of dark sky observations.
- Comparison with literature [2].

Fig. 10 shows the two dark signal non-uniformity (DSNU) spectra, normalised with respect to their mean clean dark charge value. The clean dark charge is the average DC signal over a spectrometer, characterised by its temperature, assumed to be uniform. All the pixels exhibiting an abnormal behaviour ($>3\sigma$) are excluded from the computation of the average and classified as *hot pixels*. One sees the increase of the number of pixels with high dark charge level as it is also noted that there were already several pixels presenting this behaviour of high signal on ground.

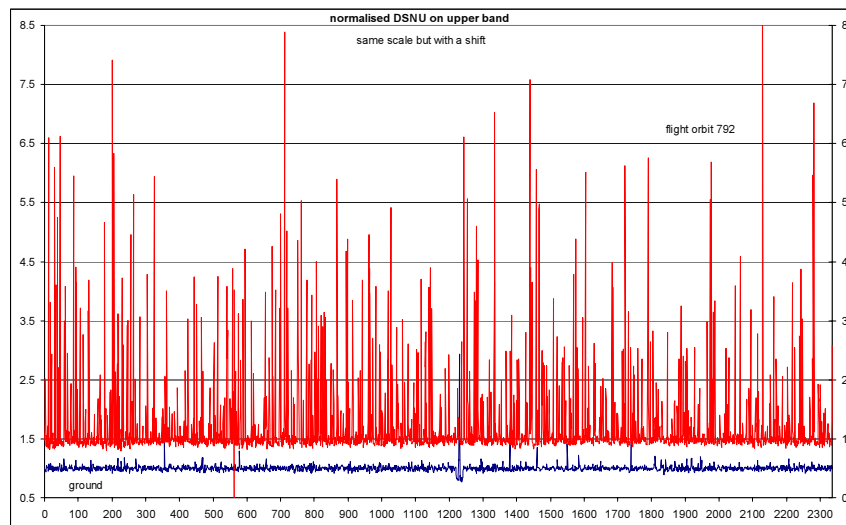


Fig. 10: DSNU before launch and two months after launch
Before (blue): left vertical axis – After (red): right vertical axis

In September 2002, 60% of the pixels have a mean dark charge higher than 100 electrons, which results in the following values displayed in the table below for all spectrometers.

Table 4: Mean dark charge per CCD

Mean DC (e)	SPA1	SPA2	SPB1	SPB2
Clean dark charge	79	80	93	92
All pixels	215	218	254	223

Using all available Dark Sky Areas observations, we derive the evolution of the mean leakage current on each spectrometer: an increase of 2.4 e/s/day at the current temperature (around -3°) is observed.

In addition to the evolution of the mean dark charge, Random Telegraphic Signal (RTS), defined as an abrupt change in the average dark charge level for a given pixel, has been observed. The observations indicate a high variability of RTS duration and stability. They have been compared to literature [2] and made appear similarities (although RTS level are higher in the present case) with published observations.

Fig. 11 presents the temporal evolution of the dark charge level of several binned pixels during a DSA observation (dark sky area). RTS events are easily visible on these curves.

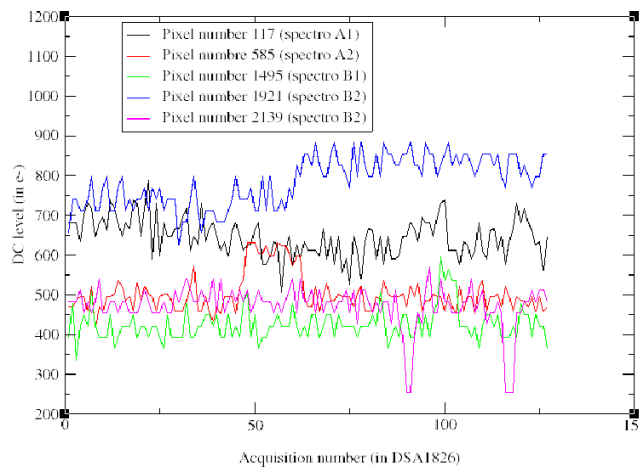


Fig. 11: RTS occurrences

Fig. 12 presents several spectra of star #018 measured outside the atmosphere (each spectrum is in fact the averaged spectrum over 10 measured spectra at the beginning of one occultation) between absolute orbits 2900 and 2920, in part of the spectral range of the spectrometer SPA2 (570-650 nm).

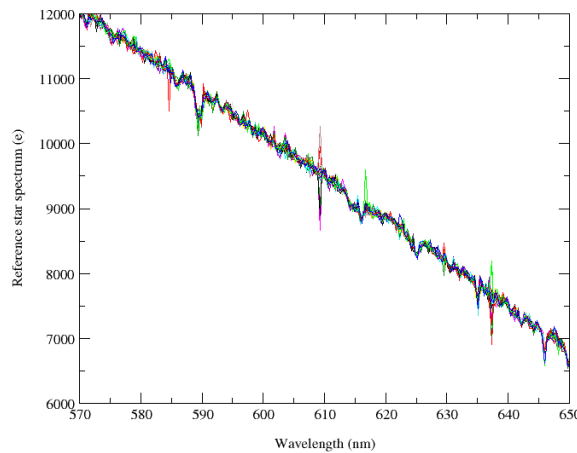


Fig. 12. : Reference star spectra (star #018, SPA2) and RTS occurrences

The analysis performed during the CAL/VAL phase has shown that 500 to 600 pixels per band (i.e. 25 percents of the samples) are affected by RTS events during one orbit (i.e. between two DC map calibrations at orbit level). The mean variation of the DC level is close to 65 electrons (1 sigma).

Fig. 13 presents an example of the temporal variation of the dark charge level due to RTS. Two dark charge maps measured at one week interval (mean dark charge around 250 e-) are compared.

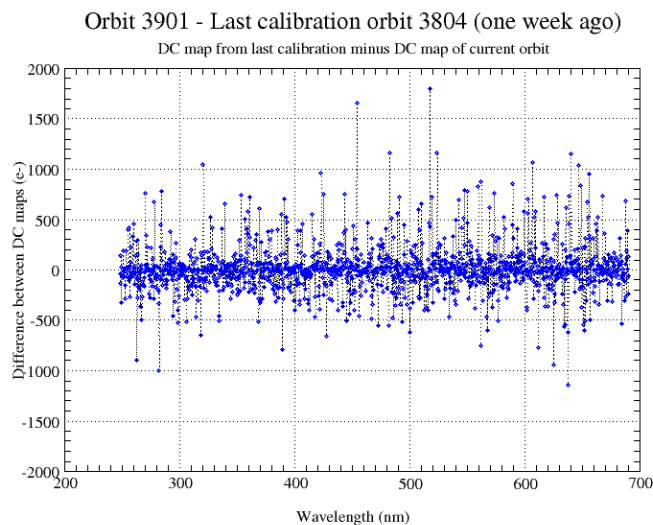


Fig. 13. : temporal variation of the DC level due to RTS

A preliminary study of the impact on the level 2 products has been performed and shows a degradation of several percents on ozone and other species. The cooling of the CCD to decrease this effect by decreasing the mean dark charge level has been performed. Anyway, the minimum temperature reached lead to a state where the RTS has still an important impact on the quality of the retrieval of several species (especially NO_2 , NO_3).

A dark charge calibration at orbit level (one DC map measured every orbit) has also been programmed and implemented in the level 1b processing chain. Using this dark charge map brings a clear improvement, of the order of a recovery of half the degradation due to RTS (conclusion reached from the analysis of a set of end to end simulations, using the GOMOS simulator, performed during the CAL/VAL activities).

1.8 Signal modulation

When analysing dark sky observations, an oscillating regular parasitic signal has been detected in addition to the dark charge:

- A modulation signal of +/-1.4 ADU has been found for spectrometer A1.
- A similar modulation signal of +/-0.76 ADU has been found for spectrometer A2.
- No modulation has been detected for spectrometers B1 and B2.

An algorithm has been prototyped to remove the modulation. It is routinely exploited for calibration analysis. Considering the improvement in the variance obtained with this algorithm, its implementation in the nominal GOMOS processing chain has been done.

The total static variance (i.e. excluding photon noise and including electronic chain noise and quantisation noise) is significantly different from the on ground values for the UVIS spectrometers when the correction for signal modulation is applied. The resulting variance for each spectrometer is given in the table below.

Table 5: Total measured static variance (i.e. excluding photon noise) in e^2

SPA1	SPA2	SPB1	SPB2
602	525	297	339
<i>Post-launch characterisation of static noise contributors after correction for modulation signal</i>			

1.9 Star spectrum location on the CCDs

The PRNU correction of the star spectra (and so of the transmission spectra) is based on a good knowledge of the location of the star spectra image on the spectrometer CCD arrays. As this information is not known in near-real time during the occultation, specific observations in spatial spread monitoring mode have been performed. The in-flight calibration has shown that this location varies with the column index (star spectrum image is slanted on the CCD array).

The next 2D figure presents the image of the star spectrum on the CCD arrays (signal is expressed in number of electrons per CCD pixel). The measurements have been performed in spatial spread monitoring mode. We analyse this map to extract the mean star spectrum location for each CCD column.

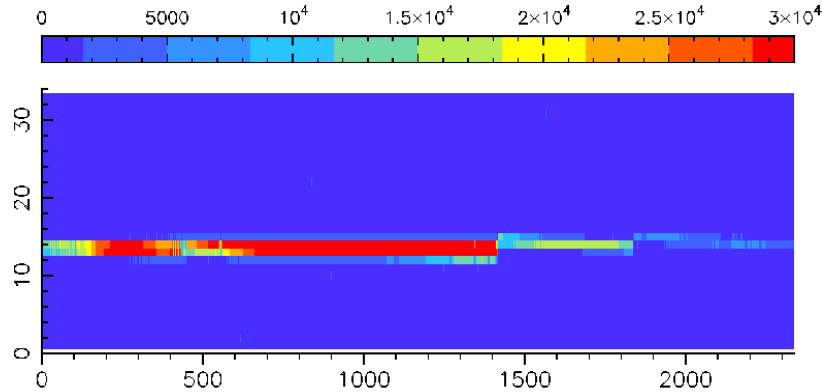


Fig. 14: Image of the star spectrum on the SPA2 CCD array

The following curve presents the mean location of the star spectrum on the spectrometer CCD arrays. This curve has been obtained from Sirius observations outside the atmosphere. As one can see, the star location is not constant on each CCD (variation greater than 1 pixel from each side of SPB1 and SPB2) but is rather a linear variation as a function of the column index. Equivalent results are observed for other stars.

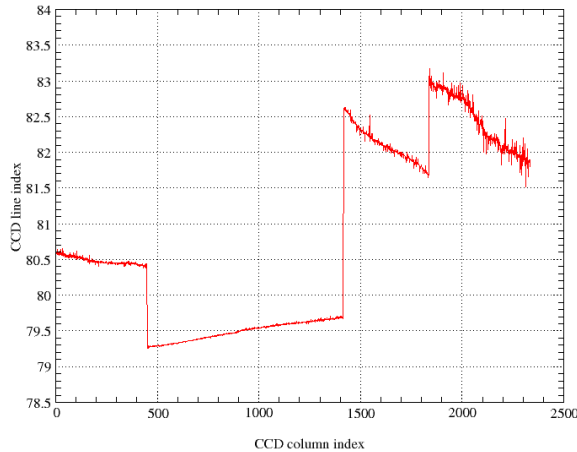


Fig. 15: Location of the maximum star signal for each CCD column (computed from a Sirius occultation in spatial spread monitoring mode)

1.10 Photometer/spectrometer intercalibration

The spectrometer measurements are used to correct the photometer measurements from limb or straylight contribution. During the calibration phase, it has been shown that the relation between the spectrometer and photometer samples were not as expected.

The consequence is that the correction quantity is not correct as soon as the tangent point altitude reaches a certain altitude. This altitude corresponds more or less to the beginning of the scintillation effects as well as the increase of mispointing errors (information provided by the SATU). Although some specific work has been produced, this behavior has not been fully understood.

Fig. 16 presents the ratio between the spectrometer and the photometer FP1 samples (SP/FP) as a function of the tangent point altitude. The spectrometer samples are integrated in the spectral range of the photometer, using the radiometric sensitivity LUT of the spectrometer (to convert the samples from electrons into physical units) and the photometer spectral transfer function (to convert from physical units into electrons). The photometer samples are averaged over a period of 0.5 seconds.

Several star occultations have been analysed for two orbits. The behavior of one star is identical for the two orbits. The difference between the stars during the same orbit seems to be due to the accuracy of the dark charge correction: some residual dark charge due to an inaccurate thermistor temperature is added to the spectrometer samples and so impacts the computed SP/FP ratio.

The expected behavior should be a constant SP/FP ratio while we observe a strong deviation below 40 km.

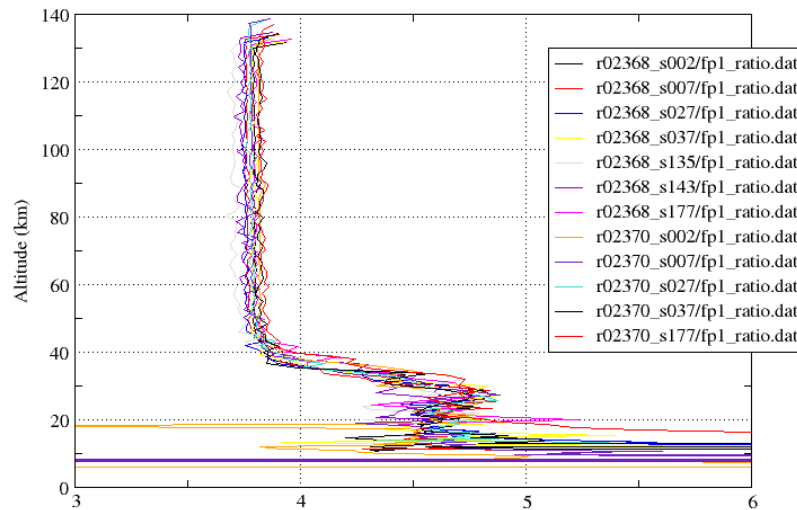


Fig. 16: Ratio between spectrometer and photometer (FP1) measured signals

The incorrect background correction has a strong impact upon the quality of the photometer data, especially in bright limb at low altitudes. The impact on the scintillation correction in the level 2 processing has not been evaluated.

1.11 Reflectivity as a function of azimuth/elevation

The reflectivity LUT is used in the level 1b processing to correct the measured star spectra (and so the transmission spectra) for reflectivity variations of the GOMOS mirror. In-flight calibration has shown that one LUT was not sufficient to describe correctly the variation of the signal with respect to the variation of elevation and azimuth angles. The calibration ADF has to be modified to handle several reflectivity LUTs. The level 1b processing has to be updated to use these LUTs. A complete reflectivity calibration has to be performed to set the different LUTs. The complexity will come from the fact that below a certain elevation, the atmosphere modifies the measured star spectrum. As a consequence, the reflectivity factor, computed as a ratio of two clean spectra, cannot be computed anymore. Some hypothesis about the variation of the reflectivity law below this elevation limit has to be made.

The following curve presents the reference star spectrum extracted from the level 1b products of several occultations covering the azimuth angular range $[-2.8^\circ; +75.7^\circ]$ for an almost constant elevation angle of 65.5° .

These spectra have been corrected from reflectivity effects with a *mean* reflectivity curve (only one LUT can be currently stored in the calibration ADF).

As one can see on Fig. 17, the correction is not perfect. One can also notice that the relative differences are not identical along the spectrum (obviously there is less difference around column 500 than around column 400 or 450).

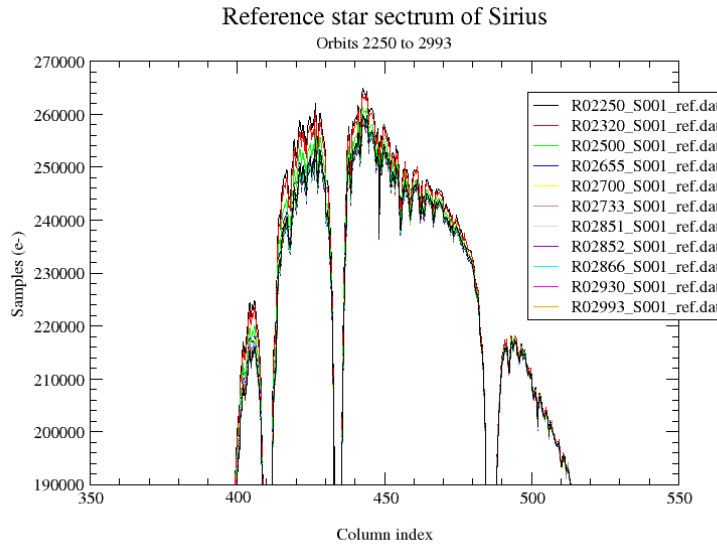


Fig. 17: Reference star spectrum of Sirius between orbits 2250 and 2993

Fig. 18 presents two reflectivity curves for spectrometer A. The X-axis is the wavelength assignment of the CCD column expressed in nm. The Y-axis is the reflectivity curve expressed in %. The pink curve corresponds to an azimuth of 54.5° while the dark blue one corresponds to an azimuth angle of 75.7° . The difference between these two curves can be of the order of 0.5%.

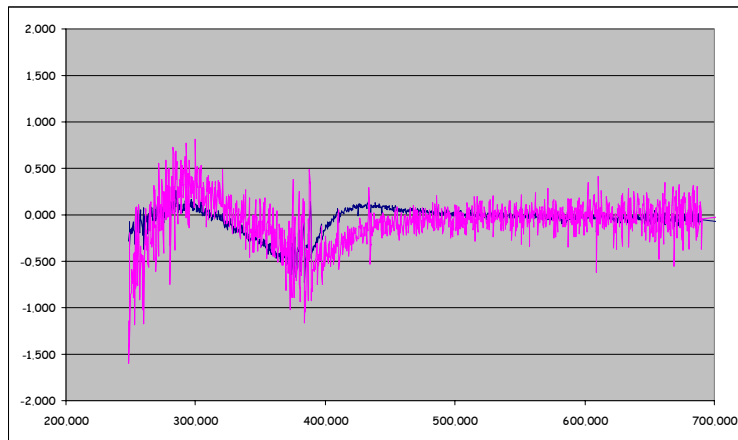


Fig. 18: Computed reflectivity factors for two SFM azimuth angles

The same effect is visible when the elevation varies for a constant azimuth angle. This is the case during any occultation. The current status leads to an error of 1% in several spectral intervals of the transmission spectra.

1.12 Background and straylight

The analysis and conclusions concerning these two items can be found in [1].

2 VALIDATED AND TUNED LEVEL 1B PROCESSING CHAIN

The main level 1b product of GOMOS is the set of geolocated and spectrally calibrated transmission absorption spectra. Fig. 19 shows an example of the transmission spectra, as extracted from a level 1b product.

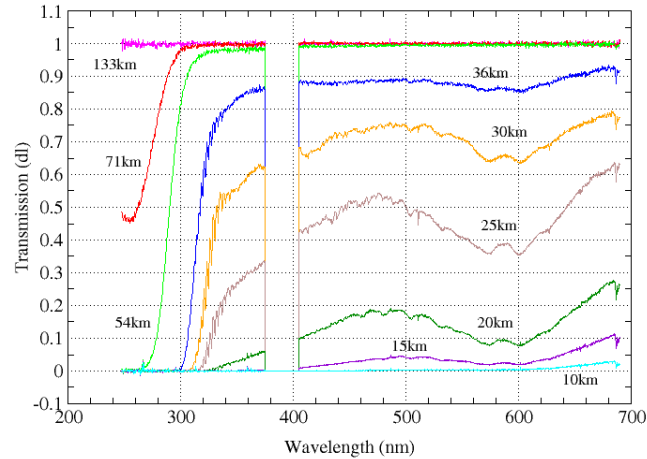


Fig. 19: Transmission – Level 1b product – Sirius occultation (29/07/2002)

Prior to calculating the transmission, the individual spectra are corrected for saturation, cosmic rays, dark charge, detector response variation (PRNU), offsets and non-linearity. The spectra are furthermore spectrally shifted using the tracking unit pointing shift data. The precise geolocation of the transmission spectra is computed, using the satellite and star positions, and a ray tracing model through the atmosphere characterised using ECMWF data combined with a climatological model above the ECMWF uppermost pressure level.

2.1 Level 1b processing step by step verification

The internal correctness of each individual processing step has been successfully checked.

2.2 Tuning of level 1b processing parameters

A second task was to tune the parameters of the level 1b processing chain in order to confirm or identify the new operational configuration. This task has led to several modifications of the Level 1b processing configuration product mostly linked to the in-flight characterisation of the instrument: suppression of the non-linearity correction, use a DC map instead of using the first measurements outside the atmosphere, cosmic rays thresholds parameters.

2.3 Upgrade of the level 1b processor and configuration parameters

During this task, the confrontation of the pre-launch defined algorithms to the real observations has shown some limitations, especially concerning the existence of an unexpected modulation signal (see dedicated chapter above), of the variation of the dark charge due to RTS events, of the detection and correction of cosmic rays and of the use of faint signal in the computation of the transmission spectra.

Modulation signal

See dedicated chapter above.

Dark charge variation due to RTS

A first corrective action has been to characterise the pixel dark charge level every orbit using a specific DSA observation. Although this correction increases the quality of the species density profile, it is intended to define and implement a more sophisticated correction step.

This new correction will probably use clean spectra stored in the GOMOS stellar spectra ADF, built from the hundreds of observations of the same star. A new task (*Cleanspec*) will handle the update of this product, using the almost one year measurements already performed by GOMOS.

Cosmic rays

Based on the analysis of the spectral and temporal variations of the signal, the algorithm led to wrong detections due mainly to the high temporal signal variations due to large scintillation acting on strong signal flux (most of the problem appeared during the processing of Sirius measurements).

In order not to incorrectly flag full transmission spectra, it has been decided on the short term to increase the cosmic ray detection threshold in the processing of the Sirius occultations. The consequence is that weak cosmic rays are no more detected now.

Fig. 20 presents the difference between consecutive measurements during the occultation of Sirius in orbit 2931 (map of signal gradient). The X-axis represents the CCD column index (the four CCDs are presented on the same graph). The Y-axis represents the measurement number. The unit is ADU. The orbit has been chosen to show real cosmic ray impacts: Envisat was inside the South Atlantic Anomaly during the observation.

In this representation, a cosmic ray is identified by a couple of red-blue points: an increase of signal due to the cosmic ray event leads to a positive gradient value (blue pixel) immediately followed by a negative gradient value (red pixel).

The long blue-red lines around measurements 140 are due to a strong variation of the signal itself and obviously not to a cosmic ray event. If the threshold for cosmic ray detection was set to 50 ADU, all these pixels are wrongly flagged as being contaminated by a cosmic ray event.

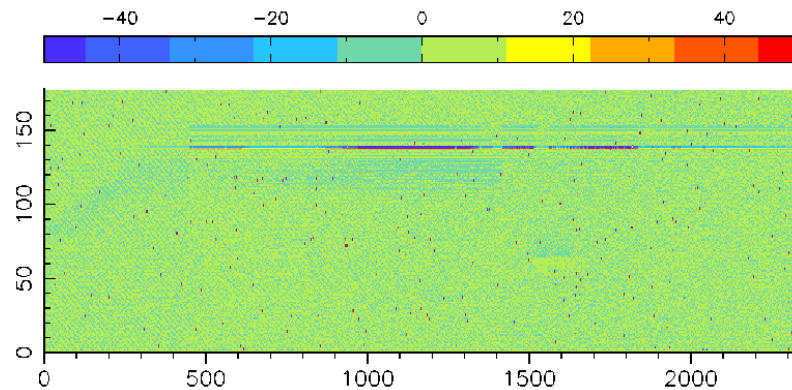


Fig. 20: Absolute difference of consecutive GOMOS measurements (orbit 2931)

With the current algorithm (only one single threshold is available), we have to choose between detecting only the strong cosmic rays and flagging large parts of spectra in case of strong scintillation.

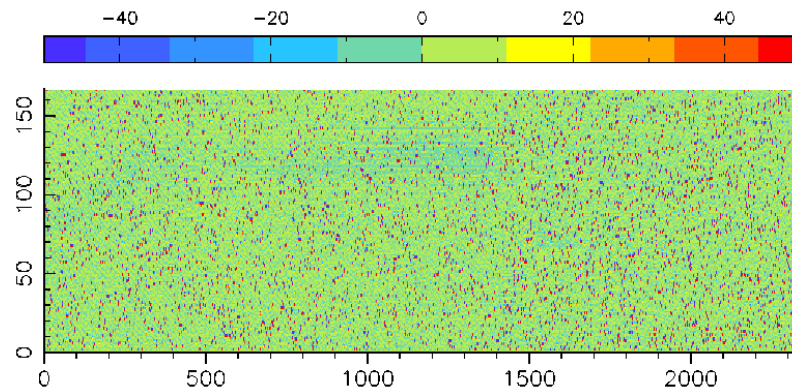


Fig. 21: Absolute difference of consecutive GOMOS measurements (orbit 2934)

A modified algorithm is proposed to take into account the averaged variations of the measurements in order to normalise them before cosmic ray detection.

Star spectra location on the CCD

As the calibration ADF contains only one line index (integer number) to define this location, it is not possible to have a very accurate PRNU correction (see dedicated chapter above).

We propose to replace the line index stored in the current calibration ADF by a LUT giving the line index as a function of the CCD column index.

As the SPB2 PRNU shows high PRNU between pixels (see the PRNU dedicated chapter above), the choice of using a constant instead of a LUT may lead to several percents of error on the star spectra after PRNU correction (i.e. also on the transmission spectra) because we will use an incorrect correction factor. This is especially true in the lower part of the atmosphere where the instrument mispointings are bigger.

SFM reflectivity factors.

As it has been shown in a previous chapter, the reflectivity factor is a function of the SFM elevation and azimuth pointing angles.

We propose to implement a reflectivity correction based upon a LUT with azimuth and elevation angles also as input parameters and not only wavelength as it is done on the current algorithm.

Reference stellar spectra

During the validation phase, it appears that the quality of the density profiles was not satisfactory in the processing of cold stars. An analysis of the star spectra and associated transmissions shows that negative star spectra combined together gave positive transmission (especially in the UV part for cold stars) taken into account in the retrieval processing.

In order to have a short-term corrective action, we have decided to apply a truncation to the reference star spectrum. The truncation has not been optimised and must be tuned and studied to estimate its impact on the retrieval quality. This threshold has to be optimised. A non-optimised threshold may lead to a loss of accuracy at high altitude for some cold stars (ozone detection is mostly based on the UV absorption at high altitude).

The current algorithm has also to be modified in order to work for example with a dynamic threshold computed from the star characteristics.

Fig 22 shows the reference star spectrum for star 52 during orbit 3060. All columns with a flux below 200 electrons (nominal threshold set in the level 1b processing configuration product) will be flagged and the corresponding transmission values are not used during the spectral inversion step in level 2 processing chain.

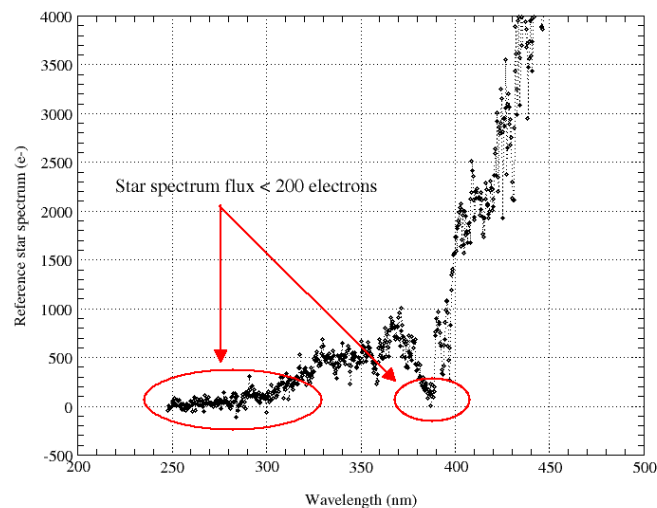


Fig. 22: Reference star spectrum (star #052 - abs. orbit 3060)

Fig. 23 shows the comparison of the transmission spectra with and without filtering of the reference star spectrum. The line is the unfiltered transmission spectrum; the blue symbols represent the filtered transmission.

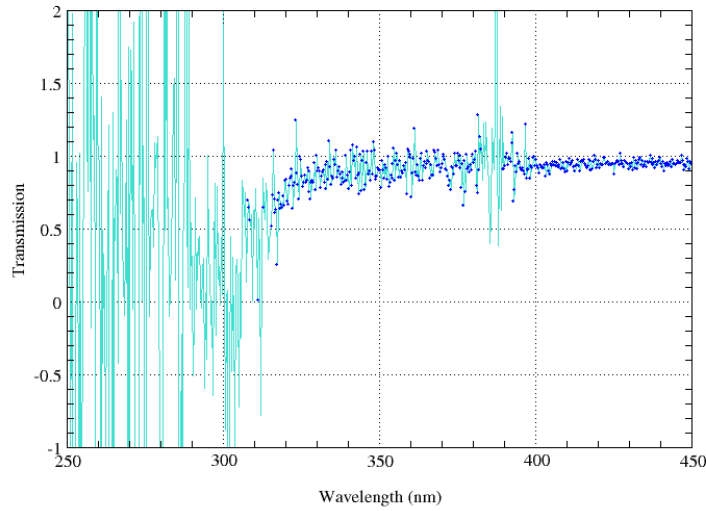


Fig. 23: Transmission with and without truncation applied

Fig. 24 presents the relative difference between the O₃ local density profiles with and without the filtering of the reference star spectrum.

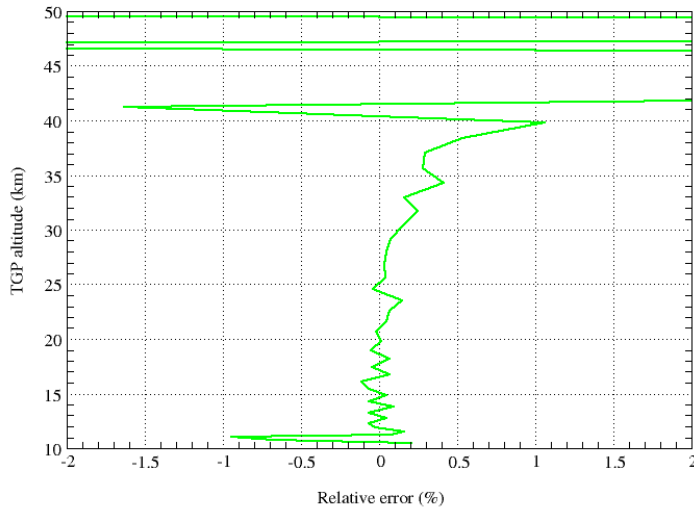


Fig. 24: Relative difference between the retrieved O₃ local density profiles with and without truncation applied

2.4 Level 1b products validation

A specific activity dedicated to the validation of the two level 1b products has started as soon as the level 1b chain was verified at module level and is still on-going at the time of the calibration review. This activity includes the verification of the data coherency, the validation of geolocation and atmosphere level 1b products, and the validation of stellar derived products. In particular, the self-coherency of GOMOS products is analysed (e.g. the instrument pointing direction and the deviation, the transmission at the same location observed by different stars, the photometer data and the spectrally integrated spectrometer data...).

3 CONCLUSIONS

Regarding the instrument operation, at the time of the validation review, the instrument operability is ready for routine phase. The altitude range may reach level down to below 5 km. The stellar magnitude range is up to 4.5.

Regarding the instrument performance, instrument in flight is within expected budget, and often better, except for CCD behaviour. The effects of each contributor to CCD behaviour have been quantified, along with their rate of evolution.

Their impact on the chain performance have made necessary some changes:

1. Three successive cooling of the CCD (orbit 800 / 1050 / 2780) down to -4°
2. New calibration procedure (introduction of regular Dark Sky Area observations)
3. Ad hoc algorithm(s) derivation for correction of the dark charge

Several algorithms of the level 1b processing chain have been specified and are currently implemented in the operational PDS system. Other actions are still under investigation:

1. Upgrade the background correction in dark (straylight) and bright conditions
2. Improve the estimation of the reference star spectrum
3. Characterise and correct for the reflectivity of the optics
4. Solve the inconsistency found in the intercalibration of spectrometers and photometers
5. Solve the non-uniformity issues for spectrometer B (re-characterisation)
6. Characterise and correct for the RTS

4 REFERENCES

1. Mangin A., et al. Limb and straylight contribution to GOMOS signal – status at end of December 2002, *ENVISAT validation workshop proceedings*, 2002
2. Proton effects in Charge-Coupled Devices, G.R. Hopkinson, C.J. Dale, and P. W. Marshall, *IEEE Transactions in nuclear science*, Vol. 43, N°2, April 1996